Magnetic Resonance Letters 2 (2022) 48–55

Contents lists available at ScienceDirect

Magnetic Resonance Letters

journal homepage: www.keaipublishing.com/MRL

Research Article

Regulation of MRI contrast and cellular retention time by cellular interfacial distribution of Gd agents: Implications for stem cell tracking

Dedicated to Professor Xiuwen Han on the occasion of her 80th birthday

Yanhui Zhang [a, b], Binbin Li [b], Bo Tan [b, *], Hailu Zhang [b, *], Zongwu Deng [a, b, *]

[a] School of Nano-Tech and Nano-Bionics, University of Science and Technology of China, Hefei, 230026, China
[b] CAS Key Laboratory of Nano-Bio Interface, Suzhou Institute of Nano-tech and Nano-bionics, Chinese Academy of Sciences, Suzhou, 215123, China

ARTICLE INFO

Article history:
Received 8 March 2021
Received in revised form 25 May 2021
Accepted 18 June 2021
Available online 12 November 2021

Keywords:
MRI
Gd agent
Cellular distribution
Relaxation rate
Intracellular retention time

ABSTRACT

Human mesenchymal stem cells (hMSCs) were labeled with Dotarem or $(Gd\text{-}DOTA)_2$- EM7 (EM7Gd2) via electroporation (EP). Cellular transmission electron microscopy (TEM) reveals free distribution of Gd agents and formation of EM7Gd2 clusters in the cytosol. Cellular magnetic resonance imaging (MRI) reveals that the free Gd agents induce MRI signal enhancement effect due to its fast exocytosis and subsequent interaction with intercellular water molecules. The EM7Gd2 clusters exhibits a longer intracellular retention time and induce a persistent MRI signal reduction effect. The cellular MRI results are interpreted by taking into account both T_1 and T_2 relaxation rates and their correlation with cellular binding structures of Dotarem and EM7Gd2.

1. Introduction

Magnetic resonance imaging (MRI) has long been pursued as *in vivo* visualization tool of cell transplants to understand its *in vivo* fates and clinical assessment of their beneficial effects [1–4]. To this goal, cells are usually labeled with a contrast agent (CA) in order to be distinguished from surrounding tissues. A long intracellular retention time (ICRT) is also required for the CA to allow the cells to be visualized over a long period. Gd agents of various structures have been pursued for labeling and imaging of cell transplants, including small molecule Gd agents, Gd-chelates coupled with dendrimers, or Gd agents embedded in liposomal nanoparticles [5–13].

Cell labeling with small molecule Gd agents is subjected to fast exocytosis of the agents as well as dilution of cellular Gd during cell division. To resolve this issue, Endres et al. developed a CA by linking Gd-DOTA to a polypeptide containing a disulfide bond, which facilitated cell penetration. Upon cell internalization, the disulfide bond is cleaved, leading to promoted

* Corresponding authors:
E-mail addresses: btan2012@sinano.ac.cn (B. Tan), hlzhang2008@sinano.ac.cn (H. Zhang), zwdeng2007@sinano.ac.cn (Z. Deng).
Peer review under responsibility of Innovation Academy for Precision Measurement Science and Technology (APM), CAS.

https://doi.org/10.1016/j.mrl.2021.100024

ICRT of the CA [5]. Nejadnik et al. developed a caspase-3 responsive Gd agent to report apoptosis of cell transplants in arthritic joints. After intravenous injection, the agent was cleaved by caspase-3 released by apoptotic cell transplants, followed by self-assembling into Gd-containing liposomal nanoparticles that could induce T_1-weighted signal enhancement at the site of apoptotic cells [6].

All these strategies make use of the T_1-weighted enhancement effect of Gd agents. Recently, we have reported that labeling hMSCs via electroporation can induce intracellular clustering of a small molecule $(Gd\text{-}DOTA)_i$-TPP (TPP, triphenylphosphonium) agent which allows tracking of the labeled cells under T_2-weighted MRI for a long period [14]. These cited works have used Gd agents of various structures and labeling strategies, which yields MRI results of different contrast (signal enhancement or reduction) and persistence (short or long). The observed difference in MRI contrast and its persistence manifests different interfacial interactions between the Gd agents and the labeled cells. Hence, a full understanding of the interfacial interactions between Gd agents and labeled cells is critical for the development and optimization of MRI CAs for *in vivo* tracking of cell transplants over long periods. From previous works, we found that MRI CAs have the ability to bind to cell membrane may cause MRI signal reduction and longer ICRT[14,15]. Hence, we selected Glu-Pro-Leu-Gln-Leu- Lys-Met (EM7) reported to targete specifically to MSCs [16] coupled with DOTA to study on how different cellular binding structures of Gd agents accelerate the relaxation processes of cellular water protons which leads to the observed MRI contrast.

2. Experimental

2.1. Synthesis of $(Gd\text{-}DOTA)_2$-EM7 (EM7Gd2)

Chemical structure of EM7Gd2 used in this work is illustrated in Fig. 1a. The EM7Gd2 complex was prepared by coupling EM7 with two Gd-DOTA complexes (Scheme S1, Text S1). More information on synthesis and characterization of the Gd-DOTA-peptide agents can be found elsewhere [14,17,18].

2.2. Aqueous relaxivity of EM7Gd2

After EM7Gd2 dissolved in ultrapure water at predetermined concentrations, longitudinal (T_1-) and transverse (T_2-) relaxation times of the samples were measured immediately on a Bruker AVANCE 500WB spectrometer (Bruker Biospin, Germany) at probe temperature of ~22 °C with Dotarem as a control. The experimental parameters are given in the ESI (Text S3).

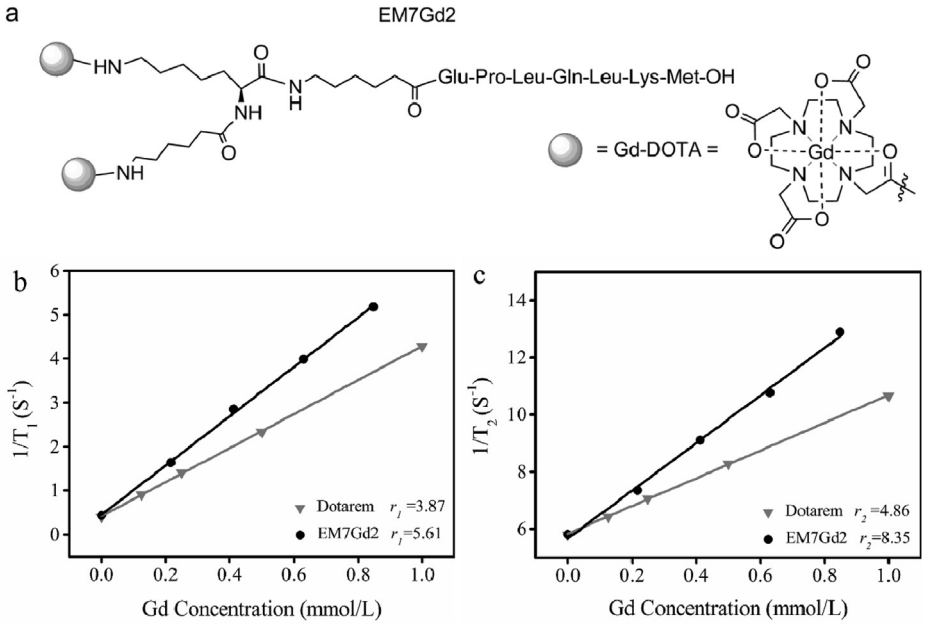

Fig. 1. (a) Chemical structure of EM7Gd2 used in this study. Aqueous (b) T_1-and (c) T_2-relaxation rates as a function of Gd concentration for Dotarem and EM7Gd2.

2.3. hMSCs culture

hMSCs were cultured in DMEM-F12 medium with 10% fetal bovine serum and 1% penicillin-streptomycin in a 5% CO_2 incubator (Thermo 3111) at 37 °C. All reagents for cell culture were purchased from Hyclone.

2.4. Cell labeling

hMSCs were electroporation (EP)-labeled with EM7Gd2 as well as Dotarem for comparison. hMSCs were seeded into cell culture dishes of 100 mm × 20 mm at a density of ~1×10^6 cells/dish, and incubated for ~2 days until near confluence. hMSCs were then re-suspended and transferred to a 96-well plate. 200 μL EP-buffer containing 2.0–10.0 mmol/L Dotarem or EM7Gd2 was added into the collected and precipitated hMSCs. The cells were then subjected to six electrical pulses of 120 V and 100 μs at an interval of 1 s from an X-Porator® (Etta Biotech, China). Then the labeled cells were recovered and suspended in DMEM-F12 medium for 15 min.

The labeled hMSCs were rinsed three times with phosphate buffer solution (PBS) and transferred into capillary tubes of 1.0 mm-i.d. Then they were centrifuged at 1400 rpm for 5 min to form a cell pellet at the bottom of the tubes for MRI assessment immediately. Unlabelled hMSCs were subjected to the same procedure as control.

2.5. Quantification of cellular gadolinium

After cell counting, labeled cells were digested using concentrated nitric acid. Total Gd content was analyzed by inductively coupled plasma-mass spectrometry (ICP-MS, Thermo X Series2). Cellular Gd content was calculated by dividing total Gd content with the counted cell number. A mean value of three repetitive measurements was reported.

2.6. Cellular TEM

Cellular distribution of Gd agents was observed by Transmission Electron Microscopy (TEM, Tecnai G2 F20 S-Twin) as described in a previous work [14]. Briefly, hMSCs EP-labled with Dotarem or EM7Gd2 at 2 mmol/L were collected, washed, fixed, dehydrated and embedded to obtain a hardened cell mass. Sample sections with a thickness of 70–90 nm were prepared with Ultramicrotome (Leica UC7) for TEM observation on a copper grid. Unlabelled hMSCs were subjected to the same procedure as control.

2.7. Cellular MRI

Cellular MRI was conducted on an AVANCE 11.7T NMR spectrometer (Bruker Biospin) with a magnetic micro-imaging system. Both T_1-and T_2-weighted images and longitudinal (T_1) and transverse (T_2) relaxation time were measured with experimental parameters described in Text S2 and S3. Internal references (ultrapure water, aqueous Dotarem solution of 0.025 and 0.125 mmol/L) were used in each cellular experiment to allow quantitative interpretation of all MR signal intensities.

2.8. Cell proliferation

Cellular MRI contrast and ICRT of the Gd agents were assessed via serial cell proliferation experiments by using cellular MRI and ICP-MS analysis [14,19]. hMSCs were labeled with Dotarem or EM7Gd2 at 5 mmol/L via electroporation. The labeled cells were divided into two groups with one group for cellular MRI immediately after cell labeling and the other group for further proliferation. When the number of cells under proliferation doubled, they were divided into two groups again for another round of cellular MRI and proliferation experiments. The experiments continued till cellular MRI delivered no further change.

2.9. Cytotoxicity assessment

For assessment of cytotoxicity induced by EP-labeling of Dotarem and EM7Gd2, 1×10^5 hMSCs were suspended in 150 μL EP-buffer containing 0, 2, 5, 10 mmol/L of Dotarem or EM7Gd2, respectively. The cells were then subjected to six electrical pulses of 120 V and 100 μs at an interval of 1 s from an X-Porator® (Etta Biotech, China). After EP-labeling, the cells were collected and suspended in 4 mL DMEM-F12, rinsed three times with 2–3 mL DMEM-F12 to remove the unlabelled Dotarem or EM7Gd2, followed by being transferred into a 96-well plate to be incubated for 4 h at 37 °C. hMSCs viability of EP-labeled with Dotarem or EM7Gd2 was assessed by using a standard CCK-8 cytotoxicity assay followed by absorption measurement at 450 nm by using a microplate reader (PerkinElmer Victor X, Singapore).

3. Results and discussion

The structure of EM7Gd2 is presented in Fig. 1a and was confirmed by electrospray ionization mass spectrometry (ESI-MS). Fragments of EM7Gd2 ($C_{82}H_{136}Gd_2N_{20}O_{27}S$, exact mass 2180.8087) were found at m/z of 1091.4174 for $[M+2H]^{2+}$, and m/z of 727.9494 for $[M+3H]^{3+}$ (Fig. S1).

Aqueous r_1 and r_2 of EM7Gd2 and Dotarem are presented in Fig. 1b and c r_1 and r_2 of Dotarem are 3.87 and 4.86 $mM^{-1}s^{-1}$, in agreement with the previous report [14]. r_1 and r_2 of EM7Gd2 are 5.61 and 8.35 $mM^{-1}s^{-1}$, exhibiting an increase of 45% and 72% for r_1 and r_2, respectively, compared with Dotarem.

Cytotoxicity induced by EP-labeling of Dotarem and EM7Gd2 were assessed and the results are presented in Fig. S2 (ESI). Cell viability of hMSCs subjected to EP in the absence or presence of Dotarem (Fig. S2A) and EM7Gd2 (Fig. S2B) at 0, 2, 5, 10 mmol/L is all about 85% of control hMSCs, suggesting that the labeling conditions are tolerable for hMSCs.

Fig. 2 presents cellular MRI images of hMSCs EP-labeled in the presence of 2.0–10.0 mmol/L Dotarem or EM7Gd2 in solution. Both T_1-and T_2-weighted images are completely different for hMSCs EP-labeled with Dotarem and EM7Gd2 regardless of their equivalent cellular Gd contents. Dotarem exhibits a significant hypertensive effect under T_1-and T_2-weighted MRI as a typical T_1 CA while EM7Gd2 displays a significant hypotensive effect under T_2-weighted MRI just like a T_2-dominated MRI CA.

In order to quantitatively assess the relationship between the observed image contrast and the cellular Gd content of the two CAs, a large number of cellular MRI data are collected and compiled in Fig. 3. Fig. 3a and b presents the measured T_1-and T_2-signal intensities as a function of cellular Gd content, respectively. T_1-weighted MRI signal intensity exhibited an increase, a plateau followed by a decrease with an increase in cellular Gd content for hMSCs EP-labeled with Dotarem (Fig. 3a), in agreement with the literature reports [20,21]. The maximum signal intensity is about 3.8 times of that of control hMSCs for EP-labeling with Dotarem achieved at cellular Gd content of 1.08×10^{10} Gd/cell (Fig. 3a). T_2-weighted signal exhibited a slight increase with cellular Gd content up to ~1.5×10^9 Gd/cell for EP-labeling with Dotarem followed by a sharp decrease with a further increase in cellular load of Gd (Fig. 3b).

EP-labeling with EM7Gd2 induced no obvious T_1-weighted signal enhancement and a straight T_2-weighted signal reduction. To induce a 50% decrease of T_2-weighted signal intensity from unlabelled hMSCs, the required cellular Gd content is about 1.5×10^{10} Gd/cell for EP-labeling with Dotarem while only 1.5×10^9 Gd/cell for EP-labeling with EM7Gd2. The results indicate that to induce the same magnitude of T_2-weighted signal reduction effect, the required cellular Gd content for EP-labeling with EM7Gd2 was 10 times lower than that for EP-labeling with Dotarem. Little attention has ever been paid to the corresponding profile of T_2-weighted MRI signal of Gd-chelate CAs, but it is important for a full understanding of the fundamental MRI physics of CAs.

In order to figure out the cause of difference in MRI contrast, cellular T_1 and T_2 relaxation rates (defined as the reciprocal of the corresponding relaxation times) were also measured during cellular MRI. Fig. 3c and d presents T_1 and T_2 relaxation rates as a function of cellular Gd content. We limit the discussion on T_1 and T_2 relaxation rates to a range of cellular Gd content between 1.0×10^9–2.0×10^{10} Gd/cell because the difference in MRI is not obvious below 1.0×10^9 Gd/cell and the T_2-relaxation time reaches beyond the detection limit above 2.0×10^{10} Gd/cell. The results indicate that in this cellular Gd content range, T_1 relaxation rate is significantly accelerated by Dotarem but not by EM7Gd2; T_2 relaxation rate is accelerated by both Dotarem and EM7Gd2, but the required cellular Gd content to induce a similar magnitude of T_2 acceleration is always lower for EM7Gd2 than for Dotarem.

For spin echo MRI used in this work, T_1 and T_2-weighted MRI signal is dependent on T_1 and T_2 relaxation rates as described by the following equations[20]:

$$F_{se} \propto (1 - e^{-T_R/T_1})e^{-T_E/T_2} \tag{1}$$

where F_{se} is T_1 or T_2-weighted signal intensity, T_1 and T_2 are T_1-and T_2-relaxation time, T_R and T_E are repetition time and echo time used for the experiments. Briefly, acceleration of T_1-relaxation rate results in a signal increase (in favor of bright contrast) in both T_1-and T_2-weighted MRI, whereas acceleration of T_2-relaxation rate results in a signal decrease (in favor of dark contrast) in both T_1-and T_2-weighted MRI.

Accordingly, acceleration of T_1-relaxation rate by Dotarem (Fig. 3c) contributes to the observed T_1-and T_2-weighted MRI signal increase in Fig. 3a and b, and acceleration of T_2-relaxation rate by Dotarem at higher cellular Gd content (Fig. 3d) contributes to the subsequent T_1-and T_2-weighted MRI signal drop in Fig. 3a and b. Insignificant acceleration of T_1-relaxation rate by EM7Gd2 (Fig. 3c) is the cause of its invariant T_1-and T_2-weighted MRI signal in Fig. 3a and b, and the significant acceleration of T_2-relaxation rate by EM7Gd2 (Fig. 3d) is the cause of the straight T_2-weighted MRI signal decrease in Fig. 3b.

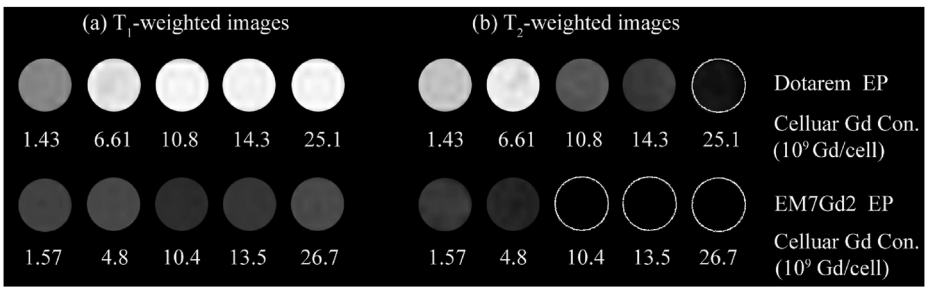

Fig. 2. *In vitro* T_1- (a) and T_2-weighted (b) MR images at 11.7 T of hMSCs EP-labeled with Dotarem (top row) and EM7Gd2 (second row) as a function of cellular Gd content. The number below each image indicates cellular Gd content in $\times 10^9$ Gd/cell. For comparison, we selected experimental data with similar intracellular Gd content between EP-labeled with Dotarem and EM7Gd2 from a large number of experimental data.

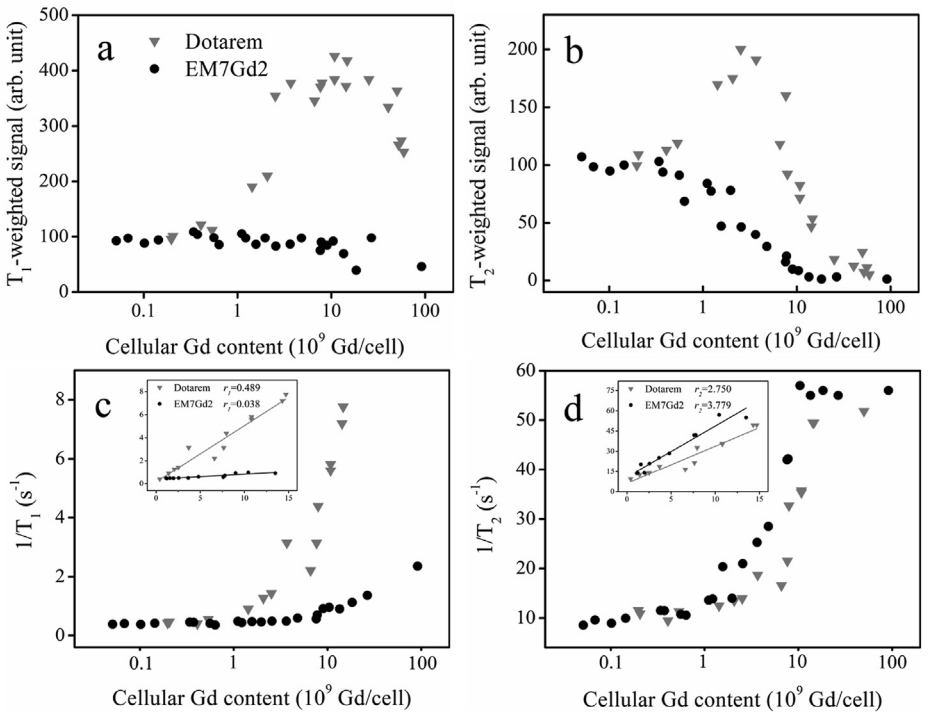

Fig. 3. T_1- (a) and T_2-weighted (b) MR signal intensity, cellular T_1 (c) and T_2 (d) relaxation rates of hMSCs EP-labeled with Dotarem and EM7Gd2 as a function of cellular Gd content. Discussion on T_2 relaxation rate has to be restricted to below 50 because the accuracy of measurement of T_2 relaxation rate deteriorates at above 50.

To further disclose the different roles on acceleration of T_1 and T_2 relaxation rates played by Dotarem and EM7Gd2, TEM was used to reveal cellular distribution of the Gd agents. Fig. 4a and b presents TEM images of control hMSCs as a reference. Fig. 4c and d presents images of hMSCs EP-labeled with Dotarem, which indicate no clustering of Dotarem either on the cell membrane or in the cytosol. It is well accepted that the introduced Dotarem is freely distributed in the cytosol [22]. Fig. 4e and f presents images of hMSCs immediately after labeling with EM7Gd2. Clustered EM7Gd2 was found on the cell membrane. Fig. 4g and h presents images of hMSCs after a 3-day recovery following EP-labelling with EM7Gd2. The EM7Gd2 clusters proceeded into the cytosol.

With the TEM observation, the underlying MRI physics of the CAs can be revealed. The significant acceleration of T_1 relaxation rate by Dotarem can be ascribed to its fast exocytosis from the cytosol and its subsequent interaction with the intercellular water molecules. This is consistent with the finding of insignificant acceleration of T_1 relaxation rate by EM7Gd2 because a much slower exocytosis and longer ICRT is expected for the formed EM7Gd2 clusters. Meanwhile, EM7Gd2 clusters induce a more severe magnetic inhomogeneity than free distributed Dotarem with the same cellular Gd content, which is in favor of acceleration of T_2 relaxation rate of both intercellular and intracellular water molecules. The findings suggest that it is

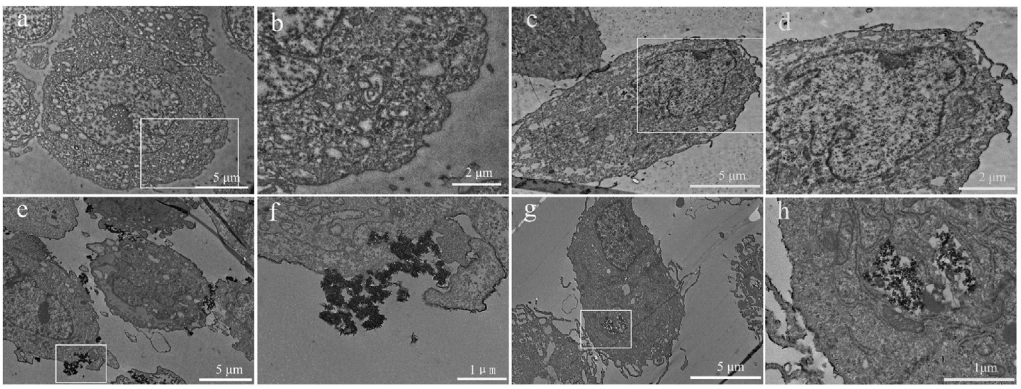

Fig. 4. TEM images of (a/b) control hMSCs, (c/d) hMSCs EP-labeled with Dotarem at 2.0 mmol/L, (e/f) hMSCs immediately after EP-labelling with EM7Gd2 at 2.0 mmol/L, and (g/h) hMSCs EP-labeled with EM7Gd2 at 2 mmol/L followed by a 3-day culture and recovery.

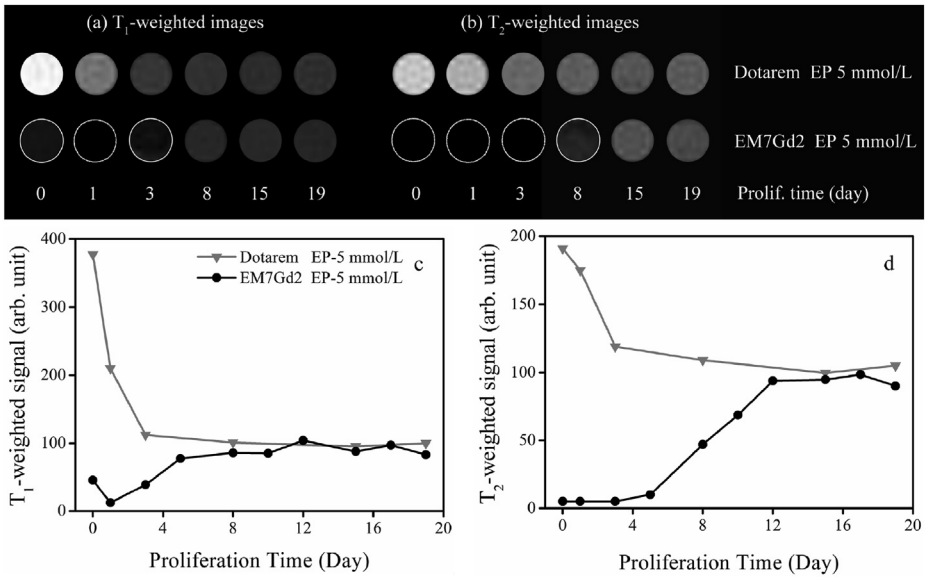

Fig. 5. Cellular T_1- (a) and T_2-weighted (b) MR images of hMSCs EP-labeled with Dotarem and EM7Gd2 at 5 mmol/L as a function of cell proliferation time. Corresponding T_1- (c) and T_2-weighted (d) MR signal intensity. T_2-weighted MR signal intensity of dark images are tentatively given a value of 5 or below for ease of following its change profile. As cellular Gd content is diluted in subsequent cell proliferation, both T_1-and T_2-weighted signal intensity of the hMSCs recovers to a value equivalent to that of control hMSCs.

critical to take into account both T_1 and T_2 relaxation rates and their correlation with cellular binding status of a CA for interpretation of CA-enhanced T_1-and T_2-weighted MRI contrast.

As a result, a persistent T_2 enhancement effect can be expected for hMSCs EP-lablelled with EM7Gd2 clusters. In order to confirm this expectation, hMSCs EP-labeled with Dotarem and EM7Gd2 were subjected to further proliferation. T_1-and T_2-weighted MRI were conducted on the hMSCs and the results are presented in Fig. 5a and b. The corresponding T_1-and T_2-weighted signal intensities are presented in Fig. 5c and d. T_1-and T_2-weighted images of hMSCs taken immediately after EP-labeling with Dotarem (day 0) exhibited bright contrast compared with control hMSCs. During subsequent cell proliferations, T_1-and T_2-weighted contrast quickly recovered (on day 3) to that of control hMSCs. On the other hand, T_2-weighted images of hMSCs EP-labeled with EM7Gd2 exhibited dark contrast compared with control hMSCs and persisted more than 10 days during subsequent cell proliferations. The finding is consistent with the expectation and implies that hMSCs EP-labeled with EM7Gd2 might be tracked for a long period under T_2-weighted MRI.

4. Conclusion

Labeling hMSCs with Dotarem or EM7Gd2 via electroporation result in different cellular interfacial distribution of the Gd agents, including free distribution of molecular Gd agents and formation of intracellular clusters in the cytosol. Gd agents in different cellular binding structures exert different acceleration effects on T_1 and T_2 relaxation rates of cellular water protons. Free distributed Gd agents are in favor of fast exocytosis and subsequent interaction with intercellular water protons, which results in significant acceleration of T_1 relaxation rate. Intracellular Gd clusters exhibit longer ICRT and cause a more severe magnetic inhomogeneity, which results in significant and persistent acceleration of T_2 relaxation rate and insignificant acceleration of T_1 relaxation rate. T_1-and T_2-weighted MR signal intensity of labeled hMSCs can be well understood with cellular T_1-and T_2-relaxation rates associated with the cellular interfacial distribution of Gd agents.

Declaration of competing interest

The authors declare no competing financial interest.

Acknowledgment

This work was funded by a general project from the Natural Science Foundation of China (21673281, 31870982) and a National Key R&D Program from MOST of China (2017YFA0104301).

Appendix A. Supplementary data

Supplementary data to this article can be found online at https://doi.org/10.1016/j.mrl.2021.100024.

References

[1] A. Gera, G.K. Steinberg, R. Guzman, In vivo neural stem cell imaging: current modalities and future directions, Regen. Med. 5 (1) (2010) 73–86.
[2] D.L. Kraitchman, J.W.M. Bulte, Imaging of stem cells using MRI, Basic Res. Cardiol. 103 (2008) 105–113.
[3] L.S. Politi, MR-based imaging of neural stem cells, Neuroradiology 49 (2007) 523–534.
[4] W.J. Rogers, C.H. Meyer, C.M. Kramer, Technology insight: in vivo cell tracking by use of MRI, Nat. Clin. Pract. Cardiovasc. Med. 3 (2006) 554–562.
[5] P.J. Endres, K.W. MacRenaris, S. Vogt, et al., Cell-permeable MR contrast agents with increased intracellular retention, Bioconjugate Chem. 19 (10) (2008) 2049–2059.
[6] H. Nejadnik, D. Ye, O.D. Lenkov, et al., Magnetic resonance imaging of stem cell apoptosis in arthritic joints with a caspase activatable contrast agent, ACS Nano 9 (2) (2015) 1150–1160.
[7] J.W.M. Bulte, T. Douglas, B. Witwer, et al., Magnetodendrimers allow endosomal magnetic labeling and in vivo tracking of stem cells, Nat. Biotechnol. 19 (12) (2001) 1141–1147.
[8] A.J.L. Villaraza, A. Bumb, M.W. Brechbiel, Macromolecules dendrimers, and nanomaterials in magnetic resonance imaging: the interplay between size, function, and pharmacokinetics, Chem. Rev. 110 (5) (2010) 2921–2959.
[9] Y. Tachibana, J.I. Enmi, A. Mahara, et al., Design and characterization of a polymeric MRI contrast agent based on PVA for in vivo living-cell tracking, Contrast Media Mol. Imaging 5 (6) (2010) 309–317.
[10] Y. Tachibana, J.I. Enmi, C.A. Agudelo, et al., Long-term/bioinert labeling of rat mesechymal stem cells with PVA-Gd conjugates and MRI monitoring of the labeled cell survival after intramuscular transplantation, Bioconjugate Chem. 25 (7) (2014) 1243–1251.
[11] J. Guenoun, A. Ruggiero, G. Doeswijk, et al., In vivo quantitative assessemnt of cell viability of gadolinium or iron-labeled cells using MRI and bioluminescence imaging, Contrast Media Mol. Imaging 8 (2) (2013) 165–174.
[12] F.J. Nicholls, M.W. Rotz, H. Ghuman, et al., DNA-gadolinium-gold nanoparticles for in vivo T_1 MR imaging of transplanted human neural stem cells, Biomaterials 77 (2016) 291–306.
[13] E.J. Ngen, L. Wang, Y. Kato, et al., Imaging transplanted stem cells in real time using an MRI dual-contrast method, Sci. Rep. 5 (2015) 13628.
[14] Y.H. Zhang, H.Y. Zhang, B.B. Li, et al., Cell-assembled $(Gd\text{-}DOTA)_i$-triphenylphosphonium (TPP) nanoclusters as a T_2 contrast agent reveal in vivo fates of stem cell transplants, Nano Res 11 (3) (2018) 1625–1641.
[15] P.L. Zhang, Y.H. Zhang, B.B. Li, et al., Cell-assembled nanoclusters of MSC-targeting Gd-DOTA-peptide as a T_2 contrast agent for MRI cell tracking, J. Pept. Sci. 24 (2018), e3077.
[16] Z.X. Shao, X. Zhang, Y.B. Pim, et al., Polycaprolactone electrospun mesh conjugated with an MSC affinity peptide for MSC homing in vivo, Biomaterials 33 (12) (2012) 3375–3387.
[17] L.M. Cao, B.B. Li, P.W. Yi, et al., The interplay of T_1- and T_2-relaxiation on T_1-weighted MRI of hMSCs induced by Gd-DOTA-peptides, Biomaterials 35 (13) (2014) 4168–4174.
[18] C. Li, P. Winnard, Z.M. Bhujwalla, Facile synthesis of 1-(acetic acid)-4,7,10-tris (tert-butoxycarbonylmethyl)-1,4,7,10-tetraazacyclododecane: a reactive precursor chelating agent, Tetrahedron Lett. 50 (24) (2009) 2929–2931.
[19] A.K. Barthel, M. Dass, M. Dröge, et al., Imaging the intracellular degradation of biodegradable polymer nanoparticles, Beilstein J. Nanotechnol. 5 (2014) 1905–1917.
[20] D.W. McRobbie, E.A. Moore, M.J. Graves, et al., in: MRI from Picture to Proton, second ed., Cambridge University Press, New York, 2006.
[21] P. Caravan, J.J. Ellison, T.J. McMurry, et al., Gadolinium (III) chelates as MRI contrast agents: structures, dynamics, and applications, Chem. Rev. 99 (1999) 2293–2352.
[22] E. Terreno, S.G. Crich, S. Belfiore, et al., Effect of the intracellular localization of a Gd-based imaging probe on the relaxation enhancement of water protons, Magn. Reson. Med. 55 (3) (2006) 491–497.

Yanhui Zhang received an M.S. degree in organic chemistry from Shanghai University in 2014. She joined the Magnetic Resonance Spectrometry and Imaging Team at Suzhou Institute of Nano-tech and Nano-bionics, Chinese Academy of Sciences (SINANO, CAS) as a research assistant, and is currently a Ph.D. candidate in Physical Chemistry at School of Nano-Tech and Nano-Bionics, University of Science and Technology of China.

Bo Tan received Ph.D. degree in Organic Chemistry from Department of Chemistry, Tsinghua University in 2000. He is currently a professor at Suzhou Institute of Nano-tech and Nano-bionics, Chinese Academy of Sciences (SINANO, CAS). His major research interests include organic chemistry and chemistry of pharmaceuticals.

Hailu Zhang received a Ph.D. degree in magnetic resonance from Wuhan Institute of Physics and Mathematics, Chinese Academy of Sciences (WIPM, CAS) in 2008. He is currently a professor at Suzhou Institute of Nano-tech and Nano-bionics, Chinese Academy of Sciences (SINANO, CAS). His major research interests include nanobiointerface physics and solid-state chemistry of pharmaceuticals.

Zongwu Deng received a Ph.D. degree in Physical Chemistry from Tsinghua University in 1999. He is currently a professor and principal investigator at Suzhou Institute of Nano-tech and Nano-bionics, Chinese Academy of Sciences (SINANO, CAS). His major research interests include MRI nanoprobes for tracking of *in vivo* fates of stem cell transplants.